Dramatic efficiency boost of single-walled carbon nanotube-Si hybrid solar cells through exposure to ppm NO_2 in air: an ab-initio assessment of the measured device performances.

Sonia Freddi,[a] *Simona Achilli,*[b, §] *Raffaella Soave,*[c] *Stefania Pagliara,*[a] *Giovanni Drera,*[a] *Andrea De Poli,*[a] *Francesco De Nicola,*[d] *Maurizio De Crescenzi,*[e] *Paola Castrucci,*[e] *and Luigi Sangaletti*[a,*]

[a] Surface Science and Spectroscopy Lab @ I-Lamp, and Dipartimento di Matematica e Fisica, Università Cattolica del Sacro Cuore, Brescia, Italy.
[b] Dipartimento di Fisica, Università di Milano, 20133 Milano, Italy.
[c] Consiglio Nazionale delle Ricerche, Istituto di Scienze e Tecnologie Molecolari and INSTM UdR di Milano, via Golgi 19, 20133 Milano, Italy.
[d] Graphene Labs, Istituto Italiano di Tecnologia, Via Morego 30, 16163 Genova, Italy.
[e] Dipartimento di Fisica, Università di Roma Tor Vergata, 00133 Roma, Italy.

ABSTRACT

We observed a 73% enhancement of the power conversion efficiency (PCE) of a photovoltaic cell based on the single wall carbon nanotube/Si hybrid junction after exposing the device to a limited amount (10 ppm) of NO_2 diluted in dry air. On the basis of a computational modeling of the junction, this enhancement is discussed in terms of both carbon nanotube (CNT) p-doping, induced by the interaction with the oxidizing molecules, and work function changes across the junction. Unlike studies so far reported, where the PCE enhancement was correlated only qualitatively to CNT doping, our study (i) provides a novel and reversible path to tune and considerably enhance the cell efficiency by a few ppm gas exposure, and (ii) shows computational results that quantitatively relate the observed effects to the electrostatics of the cell through a systematic calculation of the work function. These effects have been cross-checked by exposing the cell to reducing molecules (i.e. NH_3) that resulted to be detrimental to the cell efficiency, consistently with the theoretical *ab-initio* calculations.

INTRODUCTION

Recent investigations on hybrid carbon nanotube-silicon (CNT/Si) junctions have shown that the performances of CNT/Si photovoltaic (PV) cells can be strongly affected by exposure to selected molecules aimed to produce a chemical etching of the device interface and steer the formation of a SiO_x buffer layer, or a doping of the CNT layer.[1-10] Due to the sensitivity of electrical parameters to a flux of molecules over the CNT layer, it has also been suggested that these heterojunctions can act as sensing devices hopefully combining the sensing capability with power generation of the junction,[11-17] ultimately leading to self-powered devices.[12,18,19]

In a CNT/Si PV cell, CNTs represent both the surface of the system and part of the interface with the silicon wafer. At the surface, CNTs can interact with target gas molecules which can affect the CNT layer resistivity depending on the characteristics of these molecules. For instance, reducing molecules such as NH_3 donate electrons to p-type CNTs, which then display a resistivity increase. Consistently with this scheme, a resistivity decrease is observed upon exposure to oxidizing molecules such as NO_2.[20,21] In addition to this, CNTs are also involved at the interface with Si. Therefore the target gas molecules, that are able to reach the interface diffusing through the voids of the CNT bundle layer, can in principle affect the characteristics of the heterojunction and, as a consequence, the PV cell operation.[22] It has also been shown that the complex mechanism responsible for the high PCE reached on CNT/Si heterojunction solar cells involves the formation of hybridized C-O-Si interface states.[23] In particular, the presence of trap states originating by the C-O bond for the electrons excited in the silicon has been proved to be crucial for the design of a device as efficient as a conventional p-n silicon solar cell.

A preliminary investigation on CNT/Si based devices has shown the sensitivity of the cell performances at both NO_2 and NH_3 exposure, where NH_3 resulted to be detrimental to cell efficiency, while NO_2 resulted to improve the PV cell performances (+28% power conversion

efficiency increase, although starting from a quite low PCE value below 1%).[13] These investigations suggested that a CNT/Si junction can be operated as both a PV cell and a room temperature (RT) gas sensing device, with performances that can outperform those of a PV cell and a gas sensor alone. In this framework, the use of gas adsorption to increase the PCE deserves further consideration and a systematic approach.

So far, an increase of the PCE has been obtained by doping the p-type CNT layer through a variety of methods which include treatments with HNO_3 [24,34,35] and $SOCl_2$ [25] or with $AuCl_3$,[26-30] the deposition of a redox couple such as $CuCl_2/Cu(OH)_2$,[31] or metallocens.[32]

The main goal of these methods, relying on either molecule physisorption or chemisorption, is to increase the CNT p-doping, thus giving rise to a larger number of electrons at the system Fermi level and to a greater work function. The former effect translates into an increase of the ratio of the conductivity to optical transmittance, thus allowing thinner, more transparent CNT layers to be used and, ultimately, a larger fraction of photons to reach the heterojunction. The control of the work function of the CNTs plays, instead, a fundamental role in tailoring the CNT/Si heterojunction performances. This translates in an improvement of the solar cell characteristics in terms of increased open circuit voltage (V_{OC}) and short circuit current (I_{SC}). Up to now, the strong correlation between CNT doping and the solar cell PCE has been reported mainly qualitatively from an experimental point of view.

In the present study, we address this issue both in an experimental and theoretical framework with the aim to quantitatively correlate the amount of physisorbed molecules to the changes in the CNT work-function and, as a consequence, in the solar cell parameters, i.e. I_{SC}, V_{OC} and peak power (P_{max}). To achieve this goal, we considered a high efficiency CNT/Si PV cell which is operated during the exposure to controlled amount of gas containing NO_2 or NH_3 molecules. The device performances are tracked in real time in terms of changes of I_{SC}, V_{OC} and P_{max} upon a gas exposure. It is found that the exposure to a few ppm of NO_2 dramatically improves the cell performances with

a nearly 2-fold (i.e.73%) increase of cell PCE, from 5.6% to 9.7%. Differently, the exposure to a few ppm NH_3 is detrimental for the cell performances leading to a decrease of PCE, consistently with the reduction of charge carriers determined by the interaction of the reducing NH_3 molecules with p-doped CNTs. Ab-initio calculations of the molecule-CNT electronic density of states allowed us to discuss, in particular for NO_2 exposure, how the solar cell PCE improvement is related, through the molecule-CNT charge transfer, to a remarkable V_{OC} and P_{max} increase, and to the appearance of trap states that, hindering the e-h recombination, favor the hole transfer through the heterojunction.

MATERIALS & METHODS

Device preparation

The PV cells were prepared by depositing through dry-transfer printing [33-35] a polychiral single-walled carbon nanotube film obtained as described in ref. [35] on HF-etched 3 mm x 3 mm bare Si window delimited by a SiO_2(300nm)/Cr(5nm)/Au(150nm) electrode. The Si substrate (150 μm thick) is n-type (ρ~3-12 Ωcm, N_D~6x10^{14} cm^{-3}) with a Cr/Au ohmic back contact. Therefore, the device active area is 0.09 cm^2. The present cell belongs to a batch of devices with PCE peaked at 7.6%.

Gas exposure

NO_2 or NH_3 gases were fluxed mixed with dry air inside a vacuum-tight chamber. The inlet flux was 100 sccm of NO_2, diluted in dry air. The maximum NO_2 concentration was (10.0 ± 0.8) ppm. During the exposure the chamber was maintained at a temperature of 22 ± 1 °C and relative humidity R.H. = 25.6 ± 0.1 %. For NH_3 diluted in dry air the inlet flux was 50 sccm. The maximum NH_3 concentration was 47.1 ± 1.2 ppm. Exposure was carried out at T = 21 ± 1 °C and R.H. = 25.6

± 0.1 %. Exposure to gases was carried out in a sealed chamber, with a volume of 2 liters, equipped with an optical window and connected to a mass flow controller system, providing a stable flux of the required gases.

Current-Voltage curves and PCE measurements

PCE is defined as the ratio between the maximum power density, P_{max}, delivered by the cell and the incident light power density, $PCE = P_{max}/P_{in}$ and its value is obtained by collecting the current-voltage (I-V) curves of the device upon illumination and evaluating the open circuit voltage V_{OC}, the short circuit current I_{SC}, and P_{max}. The ratio $P_{max}/V_{OC}I_{SC}$ defines the fill factor (FF) of the cell and describes the squareness of the I-V curves in the fourth quadrant. Therefore, the performances of the cell and its PCE depend crucially on FF through:

$$PCE = FF\ V_{OC}\ I_{SC} / P_{in}.$$

In the following, only the fourth quadrant of the I-V curves will be reported, multiplied by -1.

The PCE of the PV device was measured just after the cell preparation by an AM1.5G solar simulator operating at 100 mW/cm^2 and with a spectral range peaked around 500 nm. The PCE value was 7.6%.

PCE measurements of the device inside the vacuum-tight chamber were performed by collecting current-voltage curves under illumination of a halogen lamp with a power density of 11.4 mW/cm^2 and a spectral range centered around 800-900 nm. The light from the source was focused through a lens and passed through a glass viewport to reach the cell mounted inside the chamber. The baseline PCE was in these conditions equal to 2.9%. The reduction with respect to the initial values is due to the choice of a different source and to the chamber glass window, both required to carry out the experiment with NO_2 in a sealed chamber for safety reasons. Extrapolation of the PCE value up to 100 W/cm^2 (see **Figure S1** of Supplementary Information for details) yields an estimated PCE of 5.6%, in line with the value measured just after the cell fabrication (7.6%) if we consider the

different spectral profile of the light source. In the following, we will focus on relative variations of PCE induced by exposure to gas more than on absolute values.

Theoretical calculations

The density functional theory with gradient approximation [36] for the exchange and correlation functional has been exploited throughout the ab initio simulations. We adopted a localized orbital basis set and a pseudopotential description of the core electrons, as implemented in the SIESTA package,[37] which allows us to account for hundreds of atoms in the simulation, as required by our study of the electronic properties of the system as a function of the molecule concentration.
Dispersion forces of the Grimme type [38] were included between the molecules and the CNT in order to account for van der Waals interactions. We used a double-polarized basis for all the atoms and an energy mesh cut-off equal to 350 Ry. The surface of the Brillouin zone has been sampled with 10 independent k-points in the self-consistency, whereas for the calculation of the projected DOS (PDOS) a 60-times denser mesh has been chosen. The convergence criterion for the forces has been set to 0.04 eV/Å in the atomic relaxation processes that involved only the adsorbed species. In all the calculations, the armchair (7,7) single-walled CNT has been considered, in analogy with a recent study of our group.[23] The CNT film has been simulated considering a freestanding CNT doped with oxygen atoms and adopting a separation between aligned tubes of ~60 Å along the directions perpendicular to the CNT axis. We focused here on the effect of the adsorbed molecules on the electronic properties of CNT. For this reason the interaction with the silicon substrate has been neglected. The relaxed geometry has been determined for the system with one molecule every 84 carbon atoms, corresponding to three CNT unit cells (28 atoms each one). For the other densities considered the molecular geometry and the distance from the tube has been replicated for all the molecules included in the calculation.

The smallest and the largest concentrations considered correspond to one molecule over 18 CNT unit cells, and to 7 molecules every 3 CNT unit cells, respectively. The molecules are placed in a symmetric way around the tube, progressively covering the half surface which is supposed to be exposed to the gas flux. The molecular density is defined in the following by considering only the surface available for adsorption, i.e. half nanotube, giving as extremes of variation 0.004 mol/C atom and 0.16 mol/C atom. We assumed no penetration of the molecules through the bundles forming the CNT film. The largest concentration here considered corresponds to half-nanotube completely covered, with the molecules staggered along the armchair direction and placed at a distance of one lattice vector. In this sense, the largest concentration here reported can be regarded as the saturation condition i.e. the limiting condition in which the number of molecules interacting with the tube is as large as possible. In this framework we are able to show the effect of the molecule adsorption on the work function of the nanotube. Furthermore, we are able to evaluate the charge transferred between the CNT and the molecules, as far as the molecules are absorbed on the CNT walls, although the dynamical processes leading to the adsorption-desorption of the molecules are not taken into account.

RESULTS

PV cell behavior during exposure to NH_3 and NO_2.

The behavior of the PV cell upon exposure to NO_2 is shown in **Figure 1a**. As can be observed, the exposure to NO_2 determines an increase of both I_{SC} and $V_{OC,}$ as indicated by the red arrow. In addition, also the shape of the I-V curve distinctively changes, as the I-V curve after 3 hrs exposure displays a higher FF, which leads to an overall increase of P_{max}. It is remarkable to observe that the I-V curve collected after 24 hrs in dry air (black dashed curve), i.e. with the chamber evacuated from NO_2 and left in dry air for the following 24 hours, does not recover to the starting condition, as it maintains higher V_{OC} and I_{SC} values. For comparison, in **Figure 1b**, that shows the I-V curves

collected during the NH_3 exposure (red arrow), an overall decrease of I_{SC} and V_{OC} is evident. The NH_3 exposure was started after the 24-hours period in dry air mentioned above (black dashed curve in **Figure 1b)**.

These results suggest that the NO_2 effect is twofold. The first effect is the active role of NO_2 in improving the quality of the interface in a quasi-irreversible way. This effect persists for a long time (usually several days) after the NO_2 exposure. It is known that the cell performances improve when an optimized oxide layer thickness is present at the interface between silicon and CNT.[39] A route to obtain this optimized oxide layer thickness is to remove the native silicon oxide at the CNT/Si interface by etching the cell surface in HF vapors and then exposing it to HNO_3 vapors.[35] Here the NO_2 exposure appears to affect the cell performances in a way similar to that observed after HNO_3 vapor exposure. [39]

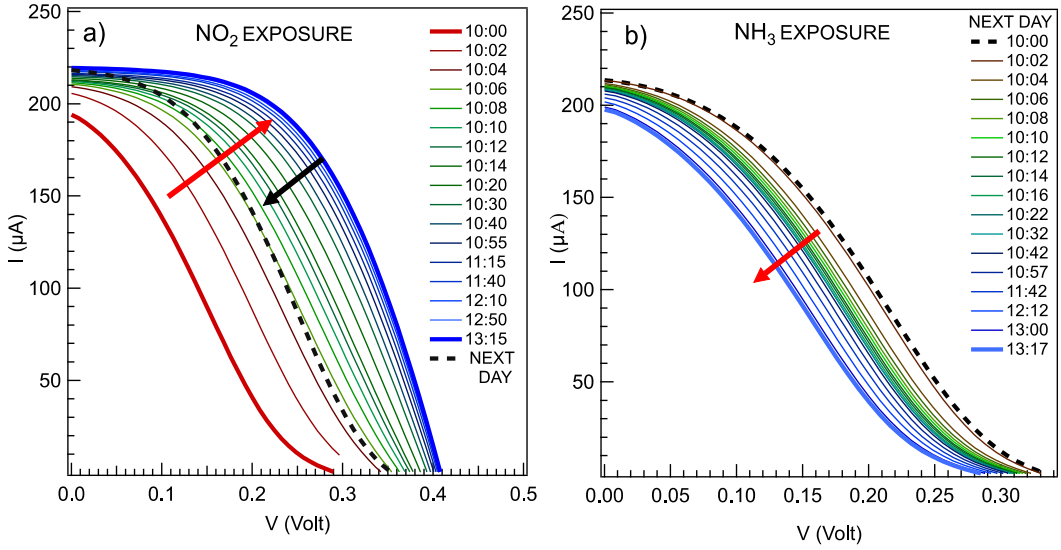

***Figure 1**: I-V curves collected at different delay time upon NO_2 a) and NH_3 b) exposure. The red arrow indicates the progression of the I-V curves during the exposure, while the black arrow points out the difference between the last I-V curve and the one collected 24 hrs after the end of the NO_2 exposure.*

The restoring of the initial PCE, as a consequence of the on-off cycle upon exposure to NO_2 atmosphere, of a cell with an already optimized SiO_x interface layer thickness (see **Figure S2** in the

Supplementary Information), confirms our claim and, at the same time, highlights the other, reversible, effect of the NO_2 molecules on the device performances. This second positive effect is also responsible of the cell performance improvement denoted by the difference between the two end-points, i.e. the dashed black and the thick blue I-V curves in **Figure 1a**. We tentatively ascribe this behavior to an additional p-doping of the CNTs and to the modification of the potential barrier at the interface.

Restoring, at room temperature, the initial condition (black dashed line in **Figure 1a,** or black thick line in **Figure S2 of the** Supplementary Material) can require several hours (about 24 hrs in the present case) as this process includes a slow purge of the chamber to reset the clean, dry air, atmosphere. In addition to this, the length of this process could be related to the presence of different covalently bound chemical groups on the CNT surface, which is likely to occur due to the strong chemical reactivity of the free radical NO_2 molecule. The reaction between NO_2 and the CNT surface can produce manifold products,[40,41] especially if defects are present on the exposed area of the CNT.[42,43] With respect to the physisorbed molecules, the chemisorbed groups are more tightly adsorbed on the CNT.

In **Figure 2** the main parameters I_{SC}, V_{OC}, P_{max} are plotted as a function of the exposure time up to the point when the chamber was saturated with NO_2 (left panels) and NH_3 (right panels). In addition to the increase of I_{SC} and V_{OC} upon NO_2 exposure and the decrease of I_{SC} and V_{OC} upon NH_3 exposure, the overall decrease of P_{max} during the exposure to NH_3 and the dramatic increase of P_{max} upon NO_2 exposure are clearly detectable. For NO_2 exposure, the cell parameter values measured the day after the NO_2 exposure are also shown, indicating that while the I_{sc} increase is preserved, the V_{oc} almost recovers the starting value.

In addition to record the extreme sensitivity of the cell parameters to the gas exposure, we observe that an increase of P_{max} determines an increase of the cell efficiency PCE, as all the measurements in the vacuum tight chamber have been carried out under the same condition of illumination,

specified in the Materials & Methods Section. This effect is even more remarkable as the final concentration of NO_2 is about 1/5 of the final concentration of NH_3 (i.e. 10 ppm NO_2 vs. 47.1 ppm NH_3, see the experimental section).

For p-doped CNT, exposure to oxidizing NO_2 is expected to increase the CNT carrier (hole) density and therefore decrease the resistivity R.[21] The opposite trend is expected for reducing NH_3 molecule exposure, consistently with the observed trend in I_{SC}. Furthermore, during the NO_2 exposure, I_{SC} shows its larger variation in the quasi-irreversible part, ascribed to the interface quality improvement. The dashed black curve of **Figure 1a** suggests, in fact, that once the interface has been optimized, the NO_2 absorption affects more V_{OC} than I_{SC}. The V_{OC} change takes place also in the reversible part, strongly suggesting that it can be related to a change/modulation of the barrier at the interface due to the gas molecule absorption.

On this basis, *ab-initio* calculations on a suitable model system have been carried out in order to investigate how the molecule absorption influences the CNT/Si barrier at the interface and ultimately the V_{OC} value.

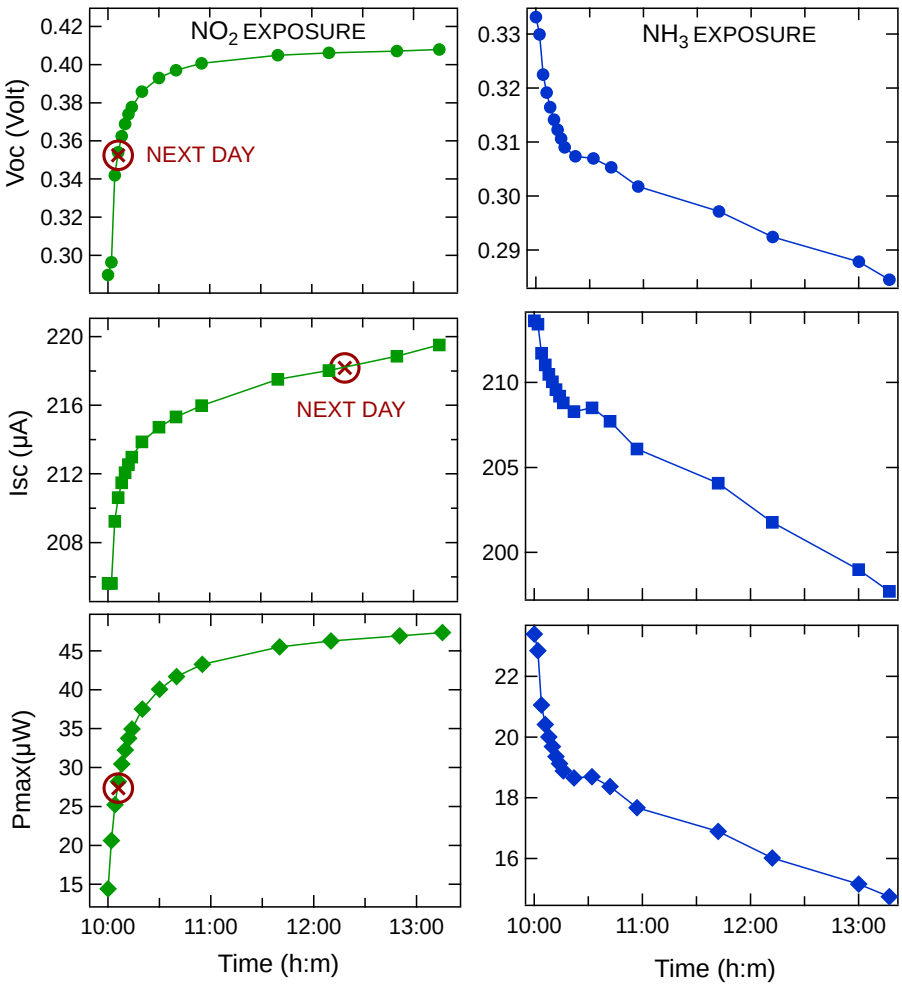

Figure 2: *V_{OC} I_{SC}, P_{max} plotted versus the exposure time for NO_2 and NH_3. The red circle indicates the parameters corresponding to the I-V curve collected the next day.*

Ab initio calculations

In order to investigate the observed impact of gas exposure on the cell parameters, first of all we determined the most stable absorption configuration for NO_2 or, alternatively, NH_3 molecules on a CNT among a number of possible configurations. To account for the interaction of the carbon nanotubes with the silicon oxide at the interface we included four oxygen atoms per CNT unit cell, staggered along the CNT armchair and zigzag directions, in bridge position with respect to two underlying carbon atoms. Hereafter, we will refer to this CNT as O-CNT. In the calculation we did not take into account the different chemical groups that could be present on the O-CNT due to the

chemical interaction with NO_2 or NH_3 molecules. The probability of the chemical reactions responsible of these strongly bound chemical groups is indeed dependent on the local geometry and thermodynamic conditions and the study of such chemical by-products is beyond the scope of this manuscript.

Among all the considered NO_2 absorption sites, detailed in the Supplementary Information, the most energetically stable configuration is that with the molecule oriented along the main axis of the O-CNT, with oxygen atoms pointing toward the O-CNT (N-up) and the N atom lying on the top of a C-C bond (see the sketches displayed in **Figure 3a).** The binding energy and other calculated relevant geometric quantities for the equilibrium configuration are reported in Table S1 in the Supplementary Material. **Figure 3b** shows the total (black line) and projected density of states (PDOS) of the O-CNT + NO_2 on the oxygen atoms at the interface (red line), on the molecule (green line) and on the CNT (blue line). The oxygen PDOS is characterized by a peak above the Fermi level (~ 0.8 eV) that can act as trap state, as already demonstrated in our previous study,[23] improving the cell performances. Differently, the molecular contribution gives a HOMO peak just below the Fermi level (-0.1 eV) and a LUMO at 2.5 eV above the Fermi level (not shown). Being the energy position of the LUMO peak considerably above the conduction band of silicon, this empty state cannot act as trap state for the electrons and consequently it cannot be the origin of the improvement of the cell performance.

In the case of NH_3 absorption on the CNT surface, the equilibrium absorption configuration corresponds to NH_3 molecules oriented with the electron-rich nitrogen atom pointing towards the nanotube and the N atom lying on the top of a carbon atom (see the sketches reported in **Figure 4a** and the values of the binding energy, the atom distances and angle in Table S1 in the Supplementary Materials).

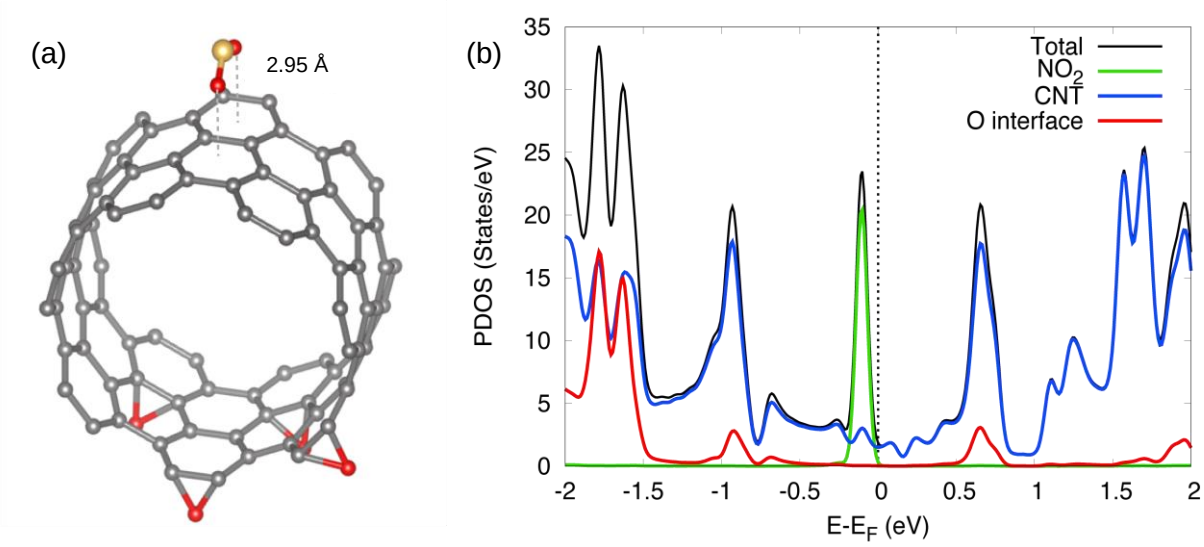

Figure 3: *(a) Equilibrium absorption configuration of O-CNT + NO_2 (b) Total (black) and PDOS on the CNT (blue line), interface oxygen atoms (red line) and NO_2 molecule (green line). The system with a molecular density of 0.024 mol/C atoms has been considered.*

In the DOS of the O-CNT + NH_3 system projected on the NH_3 molecule (see light green curve in **Figure 4b**) no states are present above the Fermi level while the energy position of the HOMO features are well below the Fermi level (~ 2 eV). Moreover, it is worth noting that the density of states at the Fermi level is slightly lower for the system with NO_2 with respect to the one with NH_3 molecule (compare the black curves of **Figure 3b** and **4b,** respectively) passing from about 1.5 to 2 states/eV.

This effect is related to the partial emptying of the CNT electronic states. Correspondingly, our calculations indicate an electron transfer of +0.118*e* and a hole transfer of -0.038*e*, being *e* the electronic charge, occurring from the CNT toward the NO_2 and NH_3 molecules, respectively. This means that for the NO_2 (NH_3) case there is an increase (reduction) of hole-carriers in the O-CNT upon molecule adsorption. Moreover, the observed charge transfer is expected to lead an increase (reduction) of the work function of the two O-CNT-NO_2 (O-CNT-NH_3) system altering the barrier at the CNT-SiO_2 interface, as explained below.

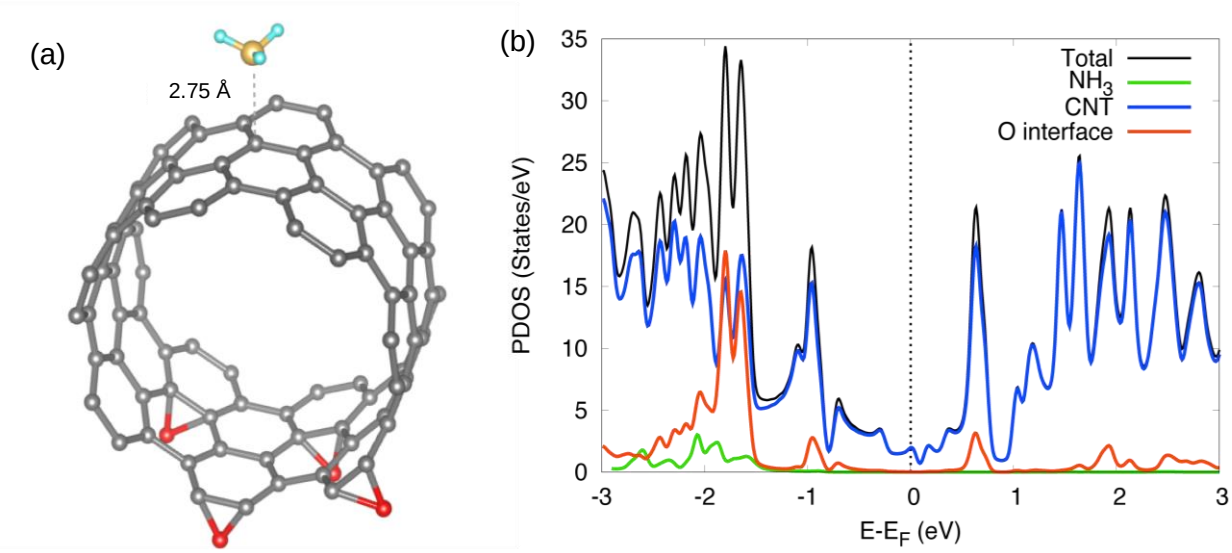

Figure 4: *(a) Equilibrium absorption configuration of O-CNT + NH_3 . (b) Total (black) and PDOS on the CNT (blue line), interface oxygen atoms (red line) and NH_3 molecule (green line). The system with a molecular density of 0.024 has been considered.*

According to the experimental results (**Figure 2**, right panel), being the improved performance mainly related to an increase of V_{OC}, we speculate that this could be explained by an increase of the interface potential barrier Φ_B.

On the basis of the theory for a Schottky junction solar cell, the V_{OC} can be indeed related to the barrier height Φ_B at the interface by the relationship:

$$V_{oc} = n\phi_B + (nkT/q)ln(J_L/A^*T^2)$$

where n is the diode ideality factor, T is the temperature, k is the Boltzmann constant, J_L is the diode saturation current density, and A^* is the Richardson constant [adapted from Ref.[44,45]].

The barrier height is calculated as the difference between the work function of the CNT film (W_{CNT}) and the silicon work function, W_{Si}, which can be determined by accounting for the Si electronic affinity (4.06 eV) and the position of our n-doped Si conduction band with respect to the quasi-Fermi level. In our case, for a dopant concentration of $N_D \sim 6x10^{14}$ cm^{-3}, the quasi-Fermi level is 0.32 eV below the conduction band, therefore the n-Si work function is ~ 4.38 eV. Thus, the change

of the work function of the nanotube through the adsorption is expected to influence the cell performances.

In order to understand if the experimental increase of efficiency in the CNT+NO_2 system is related to a variation of the work function induced by the adsorption of the molecule, we have calculated this quantity for different molecule concentrations. The work function has been extracted from the calculation by considering the asymptotic value of the Hartree potential in vacuum with respect to the Fermi level, accordingly to the definition of work function as potential barrier at the interface between the system and vacuum. In the left panel of **Figure 5**, we report the percentage of work function change with respect to the bare carbon nanotube work function, ΔW_{CNT} as a function of the density of the molecules absorbed on the CNT surface. From a rapid inspection of the figure, it is confirmed that NO_2 molecules up-shift the CNT work function (squares), while the adsorption with NH_3 has the opposite effect (triangles).

Interestingly, the variation of W_{CNT} as a function of the molecule density seems to be comparable for the two cases up to a density of 0.1. Indeed, although the amount of charge transfer is considerably smaller in the case of NH_3, the work function change is driven by the larger surface dipole of the NH_3 molecule, as compared to the NO_2 case. For the highest molecule density here considered the ΔW_{CNT} results larger for the NH_3 absorption.

The increase of the CNT work function determined by the exposure to NO_2 implies a larger band bending at the Si-CNT interface and, as a consequence, a greater V_{OC} value. In addition, as suggested, e.g., for graphene doping in graphene-silicon interfaces[46], the hole concentration at the equilibrium increases, as well as the tunneling current (**Figure 6**). The final result is an improvement of the solar cell performances. The opposite effect occurs for NH_3 doping where a decrease of the CNT work function takes place. This produces a V_{OC} reduction and an increase of the electron density at the interface, which in turn leads to an increase of the recombination probability and, ultimately yields a decrease of the light-generated current. Such results

qualitatively confirm the experimental trends of V_{OC} and I_{SC} as summarized in **Figure 5**, right panel, which shows the variation (%) of the solar cell measured parameters after the molecule longest time exposure with respect to the device initial (i.e. bare CNT) performances.

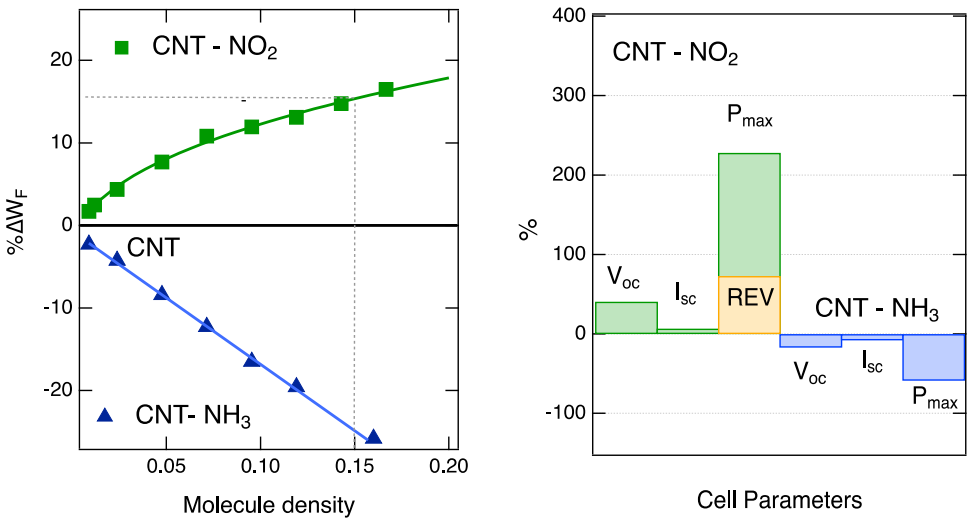

Figure 5. *Left panel: Calculated ΔW_F variations (%) vs density of molecules absorbed on the CNT surface. The molecule density is defined as the number of absorbed molecules per carbon atom belonging to the exposed CNT surface. Right panel: summary of the measured cell parameter variation following the absorption of NO_2 and NH_3. For P_{MAX} upon NO_2 absorption, the value of the reversible part (REV = 73%) is represented in yellow.*

DISCUSSION

From an experimental point of view, we observe that if the initial conditions of the solar cell are not optimal, the NO_2 exposure is able to increase the solar cell P_{max} up to 228% (**Figure 5**, right panel). If the starting solar cell efficiency is good, the P_{max} improvement due to NO_2 is of 73% and it is a totally reversible process. At the same time, the overall V_{OC} increase is of about 40%, while the reversible increase is 15%. The short circuit current grows also of a few percent. If only the reversible part is regarded, PCE measurements on a batch of cells, where the present one showed the highest PCE increase, resulted in an average PCE increase of 56.3 ± 11.1 %.

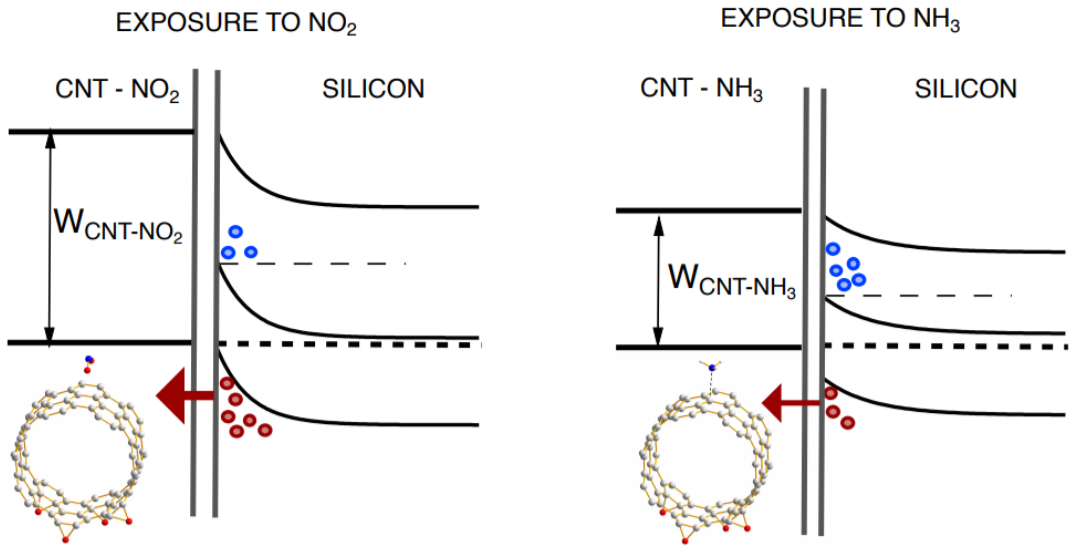

Figure 6: *Energy band diagrams of the CNT/silicon heterojunction during the NO_2 and NH_3 exposure, with an interfacial oxide layer, under illumination. The size of the red arrows indicates relative magnitudes of the photocurrent able to cross the junction. The number of circles represents the relative abundance of electrons and holes in each case.*

Finally, it is worth comparing the relative variation of V_{OC} (**Figure 2**) with the calculated ΔW_{CNT} for NO_2. Though the overall behavior of the experimental and predicted curves is consistent with each other, a comparison is rather complex. For a rough estimation of the molecule density, we have firstly measured, at the saturation, the current increase when a cell is used as a chemiresistor exposed to a of 10 ppm NO_2 concentration ($\Delta I=34 \times 10^{-6}$ A); then considering the charge transferred from the molecule to the nanotube (+0.118*e*, from the calculation) and approximating the CNT layer as an array of parallel CNTs in touch with one another, roughly corresponding to a graphene sheet completely exposed to the target gas molecules, we estimate a density of 0.15 molecules/C atom/second. This, being the density at the saturation and considering that the recovery is very slow, can be considered the density at the equilibrium (molecule/C atom). From **Figure 5a**, this value of density corresponds to an extrapolated ΔW_{CNT} of 16% which is in good agreement with the reversible V_{OC} increase (15%). This raw estimation corroborates that the main effect of NO_2 exposure on the solar cell is a change of the potential barrier at the interface.

The present results then bring the efforts to increase the PCE and the current understanding of the phenomenon beyond a mere qualitative approach, [24-33] addressing the possibility to reversibly tailor the electrostatics of the junction through the adsorption of a low and controlled amount of gas.

CONCLUSION

In conclusion, exposure to NO_2 has shown to be an efficient mechanism to dramatically increase the PCE of hybrid Si/CNT solar cells. A nearly 2-fold (i.e. 73%) PCE increase is observed upon exposure to 10 ppm NO_2. This increase can be maintained as far as the cell is operating in a mixture of dry air and NO_2. When the cell is exposed to dry air alone, the efficiency decreases to lower values. The PCE improvement is related to an increase of I_{SC}, V_{OC}, and FF. The trends observed for V_{OC} are consistent with the results of the *ab-initio* calculations carried out on a model system, which explicitly show that the absorption of NO_2 can drive the cell electrostatics and allow us to quantitatively discuss a mechanism to increase the Si/CNT cell efficiency. The experimental and theoretical results obtained for the exposure to reducing NH_3 are opposite to those obtained for the oxidizing NO_2 molecule, thus confirming our rationalization of the behavior upon gas exposure.

Corresponding Author

* luigi.sangaletti@unicatt.it

Present Addresses

§ Institut Català de Nanosciencia y Nanotecnologia, Barcelona, Spain.

Author Contributions

The manuscript was written through contributions of all authors. All authors have given approval to the final version of the manuscript.

Acknowledgements

S.F. acknowledges support from the International Doctoral Program in Science, promoted by Università Cattolica del Sacro Cuore, Italy, KU Leuven, Belgium, University of Notre Dame, USA, and Pontificia Universidad Catolica de Chile.

REFERENCES

(1) Yu, L.; Batmunkh, M.; Shearer, C.; Shapter, J. G. Use of Carbon Nanotubes (CNTs) in Third Generation Solar Cells, in Emerging Photovoltaic Materials: Silicon and Beyond, Chapt.15, S. K. Kurinec (ed.), Wiley, **2019**

(2) Tune, D. D.; Flavel, B. S. Advances in Carbon Nanotube–Silicon Heterojunction Solar Cells. *Adv. Energy Mater.* **2018**, *8*, 1703241.

(3) Yu, L.; Grace, T.; Batmunkh, M.; Dadkhah, M.; Shearer C.; Shapter, J. Insights into chemical doping to engineer the carbon nanotube/silicon photovoltaic heterojunction interface. *J. Mater. Chem. A* **2017**, *5*, 24247-24256.

(4) Li, X.; Lv, Z.; Zhu, H. Carbon/Silicon Heterojunction Solar Cells: State of the Art and Prospects, *Adv. Mater.* **2015**, *27*, 6549–6574.

(5) Castrucci, P. Carbon Nanotube/Silicon Hybrid Heterojunctions for Photovoltaic Devices. *Advances in Nano Research* **2014**, *2*, 23–56.

(6) Li, X.; Huang, J. S.; Nejati, S.; McMillon, L.; Huang, S.; Osuji, C. O.; Hazari, N.; Taylor, A. D. Role of HF in Oxygen Removal from Carbon Nanotubes: Implications for High Performance Carbon Electronics. *Nano Lett.* **2014**, *14*, 6179−6184.

(7) Pintossi, C.; Salvinelli, G.; Drera, G.; Pagliara, S.; Sangaletti, L.; Del Gobbo, S.; Morbidoni, M.; Scarselli, M.; De Crescenzi, M.; Castrucci, P. Direct Evidence of Chemically Inhomogeneous, Nanostructured, Si−O Buried Interfaces and Their Effect on the Efficiency of Carbon Nanotube/Si Photovoltaic Heterojunctions. *J. Phys. Chem. C* **2013**, *117*, 18688−18696.

(8) Tune, D. D.; Hennrich, F.; Dehm, S.; Klein, M. F. G.; Glaser, K.; Colsmann, A.; Shapter, J. G.; Lemmer, U.; Kappes, M. M.; Krupke, R.; Flavel, B. S. The Role of Nanotubes in Carbon Nanotube–Silicon Solar Cells. *Adv. Energy Mater*. **2013,** *3*, 1091–1097.

(9) Tune, D. D.; Flavel, B. S.; Krupke, R.; Shapter, J. G. Carbon Nanotube-Silicon Solar Cells. *Adv. Energy Mater.* **2012**, *2*, 1043–1055.

(10) Jia, Y.; Cao, A.; Kang, F.; Li, P.; Gui, X.; Zhang, L.; Shi, E.; Wei, J.; Wang, K.; Zhu, H.; Wu, D. Strong and Reversible Modulation of Carbon Nanotube-Silicon Heterojunctions Solar Cells by an Interfacial Oxide Layer. *Phys. Chem. Chem. Phys*. **2012**, *14*, 8391-8396.

(11) Chernov, A. I.; Eremina, V. A.; Shook, J.; Collins, A.; Walker, P.; Fedotov, P. V.; Zakhidov, A. A.; Obraztsova, E. D. Field Effect Transistor Based on Solely Semiconducting Single-Walled Carbon Nanotubes for the Detection of 2-Chlorophenol. *Phys. Stat. Sol. B* **2018**, *255*, 1700139.

(12) Liu, L.; Li, G. H.; Wang, Y.; Wang, Y. Y.; Li, T.; Zhang T.; Qin S. J. A photovoltaic self-powered gas sensor based on a single-walled carbon nanotube/Si heterojunction. *Nanoscale* **2017**, *9*, 18579.

(13) Rigoni, F.; Pintossi, C.; Drera, G.; Pagliara, S.; Lanti, G.; Castrucci, P.; De Crescenzi, M.; Sangaletti L. A cross-functional nanostructured platform based on carbon nanotube-Si hybrid junctions: where photon harvesting meets gas sensing. *Sci. Rep*. **2017**, *7*, 44413.

(14) Bai, X.; Wei, J. Q.; Jia, Y.; He, S. Q.; Sun, H. H.; Zhu, H. W.; Wang, K. L.; Wu, D. H. The influence of gas absorption on the efficiency of carbon nanotube/Si solar cells. *Appl. Phys. Lett.* **2013**, *102*, 143105.

(15) Fan, G.; Fan, L.; Li, Z.; Bai, X.; Mulligan, S.; Jia, Y.; Wang, K.; Wei, J.; Cao, A.; Wu, D.; Wei, B.; Zhu, H. Hybrid effect of gas flow and light excitation in carbon/silicon Schottky solar cells. *J. Mater. Chem.* **2012**, *22*, 3330–3334.

(16) Somani, P. R. Pressure sensitive multifunctional solar cells using carbon nanotubes. *Appl. Phys. Lett*. **2010**, *96*, 173504.

(17) Star, A.; Joshi, V.; Skarupo, S.; Thomas, D.; Gabriel, J. C. Gas sensor array based on metal-decorated carbon nanotubes, *J. Phys. Chem. B* **2006**, *110*, 21014–20.

(18) Wang, Z. L.; Chen, J.; Lin, L. Progress in triboelectric nanogenerators as a new energy technology and self-powered sensors. *Energy Environ. Sci.* **2015**, *8*, 2250–2282.

(19) Wang, Z. L.; Wu, W. Z. Nanotechnology-enabled energy harvesting for self-powered micro-/nanosystems. *Angew. Chem. Int. Edit*. **2012**, *51*, 11700–11721.

(20) Zhao, J.; Buldum, A.; Han, J.; Lu, J. P. Gas molecule adsorption in carbon nanotubes and nanotube Bundles. *Nanotechnology* **2002**, *13*, 195.

(21) Kong, J.; Franklin, N. R.; Zhou, C.; Chapline, M.G.; Peng, S.; Cho, K.; Dai, H. Nanotube molecular wires as chemical sensors. *Science* **2000**, *287*, 622–625.

(22) Hu, X.-G.; Hou, P.-X.; Liu, C.; Zhang, F.; Liu, G.; Cheng, H.-M. Small-bundle single-wall carbon nanotubes for high-efficiency silicon heterojunction solar cells. *Nano Energy* **2018**, *50*, 521–527.

(23) Ponzoni, S.; Achilli, S.; Pintossi, C.; Drera, G.; Sangaletti, L.; Castrucci, P.; De Crescenzi, M.; Pagliara, S. Hybridized C-O-Si Interface States at the Origin of Efficiency Improvement in CNT/Si Solar Cells. *ACS Appl. Mater. Interfaces* **2017**, *9*, 16627-16634.

(24) Geng, H.-Z.; Kim, K. K.; So, K. P.; Lee, Y. S.; Chang, Y.; Lee, Y. H. Effect of Acid Treatment on Carbon Nanotube-Based Flexible Transparent Conducting Films. *J. Am. Chem. Soc.* **2007**, *129*, 7758.

(25) Dettlaff-Weglikowska, U.; Skákalová, V.; Graupner, R.; Jhang, S. H.; Kim, B. H.; Lee, H. J.; Ley, L.; Park, Y. W.; Berber, S.; Tománek, D.; Roth, S. Effect of $SOCl_2$ treatment on electrical and mechanical properties of single-wall carbon nanotube networks. *J. Am. Chem. Soc.* **2005**, *127*, 5125.

(26) Jung, Y.; Li, X.; Rajan, N. K.; Taylor, A. D.; Reed, M. A. Record high efficiency single-walled carbon nanotube/silicon p-n junction solar cells. *Nano Lett.* **2012**, *13*, 95.

(27) Li, X.; Jung, Y.; Sakimoto, K.; Goh, T.-H.; Reed, M. A.; Taylor, A. D. Improved efficiency of smooth and aligned single walled carbon nanotube/silicon hybrid solar cells. *Energy Environ. Sci.* **2013**, *6*, 879.

(28) Chen, L.; He, H.; Zhang, S.; Xu, C.; Zhao, J.; Zhao, S.; Mi, Y.; Yang, D. Enhanced solar energy conversion in Au-doped, single-wall carbon nanotube-Si heterojunction cells. *Nanoscale Res. Lett.* **2013**, *8*, 225.

(29) Harris, J. M.; Semler, M. R.; May, S.; Fagan, J. A.; Nature of Record Efficiency Fluid-Processed Nanotube–Silicon Heterojunctions *J. Phys. Chem. C* **2015**, *119*, 10295.

(30) Harris, J. M.; Headrick, R. J.; Semler, M. R.; Fagan, J. A.; Pasquali, M.; Hobbie, E. K. Impact of SWCNT processing on nanotube-silicon heterojunctions. *Nanoscale* **2016**, *8*, 7969.

(31) Cui, K.; Qian, Y.; Jeon, I.; Anisimov, A.; Matsuo, Y.; Kauppinen, E. I.; Maruyama, S. Scalable and Solid- State Redox Functionalization of Transparent Single- Walled Carbon Nanotube Films for Highly Efficient and Stable Solar Cells. *Adv. Energy Mater.* **2017**, *7*, 1700449.

(32) Tune, D.; Shapter, J. Effect of Nanotube Film Thickness on the Performance of Nanotube-Silicon Hybrid Solar Cells. *Nanomaterials* **2013**, *3*, 655.

(33) Del Gobbo, S.; Castrucci, P.; Fedele, S.; Riele, L.; Convertino, A.; Morbidoni, M.; De Nicola, F.; Scarselli, M.; Camilli, L.; De Crescenzi, M. Silicon spectral response extension through single wall carbon nanotubes in hybrid solar cells. *Journal of Materials Chemistry C*, 2013, *1*, 6752

(34) De Nicola, F.; Salvato, M.; Cirillo, C.; Crivellari, M.; Boscardin, M.; Scarselli, M.; Nanni, F.; Cacciotti, I.; De Crescenzi, M.; Castrucci, P. Record efficiency of air stable multi-walled carbon nanotube/silicon solar cells. *Carbon* **2016**, *101*, 226-234.

(35) De Nicola, F.; Salvato, M.; Cirillo, C.; Crivellari, M.; Boscardin, M.; Nardone, M.; De Matteis, F.; Motta, N.; De Crescenzi, M.; Castrucci, P. 100% internal quantum efficiency in polychiral single-walled carbon nanotube bulk heterojunction/silicon solar cells, *Carbon* **2017**, *114*, 402-410.

(36) Perdew, J. P.; Burke, K.; Ernzerhof, M. *Phys. Rev. Lett.* **1996**, *77*, 3865.

(37) Soler, J. M.; Artacho, E.; Gale, J. D.; Garcìa, A.; Junquera, J.; Ordejon, P.; Sanchez-Portal, D. The SIESTA method for ab initio order-N materials simulation. *J. Phys.: Condens. Matter,* **2002**, *14*, 2745.

(38) Grimme, S. *J. Comput. Chem*. **2006**, *27*, 1787-1799.

(39) Pintossi, C.; Pagliara, S.; Drera, G.; De Nicola, F.; Castrucci, P.; De Crescenzi, M.; Crivellari, M.; Boscardin, M.; Sangaletti, L. Steering the Efficiency of Carbon Nanotube–Silicon Photovoltaic Cells by Acid Vapor Exposure: A Real-Time Spectroscopic Tracking. *ACS Appl. Mater. Interfaces* **2015**, *7*, 9436-9444.

(40) Ellison, M. D.; Crotty, M. J.; Koh, D.; Spray, R. L.; Kaitlin E. Tate Adsorption of NH_3 and NO_2 on Single-Walled Carbon Nanotubes. *J. Phys. Chem. B* **2004**, *108*, 7938-7943.

(41) Lin, T.; Bajpai, V.; Ji, T.; Dai, L. Chemistry of Carbon Nanotubes, *Aust. J. Chem*. **2003**, *56*, 635-651.

(42) Porto, A. B.; De Oliveira, L. F. C.; Dos Santos, H. F. Exploring the potential energy surface for reaction of SWCNT with NO_2^+: A model reaction for oxidation of carbon nanotube in acid solution. *Comput. Theor. Chem.* **2016**, *1088*, 1–8.

(43) Ruiz-Soria, G.; Perez Paz, A.; Sauer, M.; Mowbray, D. J.; Lacovig, P.; Dalmiglio, M.; Lizzit, S.; Yanagi, K.; Rubio, A.; Goldoni, A.; Ayala, P.; Pichle, T. Revealing the Adsorption Mechanisms of Nitroxides on Ultrapure, Metallicity-Sorted Carbon Nanotubes. *ACS Nano* **2014**, *8*, 1375–1383.

(44) Ponpon, J. P.; Siffert, P. Open-circuit voltage of MIS silicon solar cells. *J. Appl. Phys.* **1976**, *47*, 3248–3251.

(45) Chattopadhyay, P. Functional dependence of open circuit voltage on interface parameters and doping concentration of MIS solar cells. *Phys. Stat. Sol. A* **1993**, *140*, 587–592.

(46) Song, Y.; Li, X.; Mackin, C.; Zhang, X.; Fang, W.; Palacios, T.; Zhu, H.; Kong, J. Role of Interfacial Oxide in High-Efficiency Graphene−Silicon Schottky Barrier Solar Cells. *Nano Lett.* **2015**, *15*, 2104−2110.